Research Article
Volume 10:5, 2021

Journal of Material Sciences & Engineering

ISSN: 2169-0022 Open Access

Development of Antifouling Thin Film Nanocomposite Polyamide Membrane using ITO Nanoparticles

Guibin Ma*, Zayed Almansoori, Behnam Khorshidi and Mohtada Sadrzadeh*

Department of Mechanical Engineering, University of Alberta, Edmonton, Canada

Abstract

The development of nanocomposite membranes for desalination and wastewater treatment has attracted significant interest in recent years. This exceptional growth is owed to the enhanced multi functionalities of the nanocomposite membranes in terms of permselectivity, thermal stability, electrical conductivity, and antifouling propensities. In the present work, we fabricated novel thin film nanocomposite (TFN) polyamide membranes using indium tin oxide (ITO) nanoparticles. The thin film composite (TFC) membranes were synthesized by interfacial polymerization (IP) reaction using m-phenylenediamine (MPD)-aqueous solution and trimesoyl chloride (TMC)-ITO heptane solution. The addition of ITO nanoparticles to the polyamide layer significantly improved the water flux from 25.3 LMH for the pristine TFC membrane to 43.5 LMH for the ITO-modified TFN membrane with a slight reduction in salt rejection from 98% to 97% during the treatment of saline water (2000 ppm NaCl). Also, TFN membranes demonstrated superior antifouling propensity than the pristine and commercial membranes during filtration of oil sands produced water to remove organic matter. The improved fouling resistance of TFN membranes was mainly attributed to their enhanced surface wettability as the contact angle decreased from ~82° for the pristine TFC to ~65° for TFN membranes.

Keywords: Thin film nanocomposite membranes • Reverse osmosis • Polyamide • Indium tin oxide nanoparticles • Antifouling membranes

Introduction

Clean water has become a vital global commodity for many municipal, agricultural, and industrial applications due to world-wide climate change, exponential population growth, and rapid industrialization over the last decade [1,2]. It is projected that about 50% of the world's population will experience water scarcity in their living area by 2025 [3]. Furthermore, the current large dependency on conventional energy resources has exacerbated this problem as most of the energy based industries (e.g., oil and gas) require water for their activities. The current inefficient water treatment techniques enhance demands on finite freshwater resources, pushing the limits of environmental sustainability. Hence, to relieve the water shortage stress, global efforts have been accelerated to develop new technologies to produce clean water from contaminated resources [4]. Membrane based separation processes, especially reverse osmosis (RO), are proved as attractive techniques for water and wastewater treatment due to their distinct advantages over conventional methods, e.g., higher quality of permeate and smaller footprint [5]. The most broadly utilized RO membranes are thin film composite (TFC) polyamide membranes [6]. TFC membranes consist of a thin film of a polyamide film (~100-200 nm) on top of a microporous substrate [7]. Although significant advancement has been made in the development of high performance TFC membranes, there is still high interest in the fabrication of innovative membranes with enhanced permeation properties and antifouling propensity for diverse applications, including industrial and municipal waste treatment and seawater desalination [8–12]. This demand can be met by modifying the TFC membranes mainly by chemical grafting of functionalized macromolecules to the surface and integrating multifunctional nanofillers into the active polyamide layer. Nanomaterials offer several advantages like easier scale up and environmental friendliness due to the stronger entrapment of nanomaterials within the polymer matrix compared to the anchored functional materials via chemical grafting to the membrane surface. In addition, nanomaterials can substantially alter the surface and bulk physicochemical properties of the composite polymers owing to their enhanced area to volume ratio [13,14]. The first report on the modification of polymer properties with nanomaterials is a study by Paul and Kemp in 1973. They added zeolite nanofillers into polydimethylsiloxane (PDMS) polymer to improve its permeation performance for the gas separation application [15]. Later, the zeolite modified membranes were tested for water treatment by Jeong et al. in 2007. They synthesized the first polyamide thin film nanocomposites (TFN) by integrating zeolite A with the polyamide layer of a conventional TFC membrane [16]. Jeong et al. reported a substantial enhancement in water flux, with almost the same salt removal percentage as the base TFC membrane. This modification approach has become a focus for the development of novel TFN membranes with enhanced permselectivity, thermomechanical durability, electrical conductivity, and antibacterial propensity [17–20]. These functionalities have been established by the incorporation of a large family of nanomaterials, including carbon based nanofillers (such as carbon nanotubes and graphene derivatives), metal and metal oxides (such as silver and alumina), and minerals (such as silicon oxide and zeolite) [21–25]. Despite the vast number of published reports, this stream of research and development is advancing with high momentum to explore novel nano-enabled membranes for water treatment and gas separation [26–28].

Our objective in the present work is to investigate the impact of incorporating indium tin oxide (ITO) NPs into the selective polyamide film of TFC membranes on the permeation and antifouling performance of the resulting TFN membranes. Based on an earlier report by Khorshidi et al.

***Address for Correspondence:** Guibin Ma and Mohtada Sadrzadeh, Department of Mechanical Engineering, University of Alberta, Edmonton, Canada, Email: guibin@ualberta.ca and sadrzade@ualberta.ca*

Received date: 10 May, 2021; **Accepted date:** 24 May, 2021; **Published date:** 31 May, 2021

[29], the bulk integration of ITO to a polyethersulfone membrane via phase inversion method has led to the formation of nanocomposite membrane with enhanced water permeability, electrical conductivity, thermal stability, and antifouling propensity. However, the additional benefit of integrating ITO NPs within the active polyamide layer needed further investigation. To overcome the challenge of nanoparticle aggregation, we prepared a monodisperse suspension of nano-sized ITO particles in an organic solvent (heptane) through a systematic study of eight dispersion parameters [30]. The stable ITO suspension was added to the organic monomer solution and used to synthesize polyamide film via interfacial polymerization reaction [30]. Various surface and bulk characterization techniques were used to evaluate the structural morphology, permeability, and physicochemical characteristics of the membranes. The fouling resistance of the membranes was also assessed by the filtration of process-affected water generated in Canada's oil sands industry.

Materials and Methods

Materials

$InCl_3$ and $SnCl_4$ were purchased from Strem Chemicals Inc. (MA, USA). BYK-106 dispersing chemical was purchased from ALTANA (Wesel, Germany). Polyethersulfone (PES) microfiltration membrane was obtained from Sterlitech Co. (WA, USA). 1,3-Benzenediamine (MPD), 1,3,5-Benzenetricarbonyl trichloride (TMC), ammonium hydroxide (NH_4OH), triethylamine (TEA), camphorsulfonic acid (CSA), and sodium dodecyl sulfate (SDS) were all supplied from Sigma Aldrich (USA). Fouling tests were conducted using the produced water of steam assisted gravity drainage (SAGD) operation, a common bitumen recovery method in Alberta, Canada. In the SAGD process, steam is pumped to the production well to lower heavy oil viscosity and facilitate the recovery process. To recycle the process affected water and minimize freshwater consumption, the produced water is treated by a series of chemical treatment methods, including warm lime softener (WLS) and ion exchange (IX) resins [31–34]. Table 1 presents the main properties of the WLS inlet water.

Parameter	Value
pH	9-10
TOC (ppm)	450-500
TDS (ppm)	2300-2800
Conductivity (µS/cm)	1800-2200
Na^+ (ppm)	400-480
Mg^{2+} (ppm)	0.6-0.8
Ca^{2+} (ppm)	1.5-1.8
Silica, dissolved (ppm)	90-130

Table 1. Properties of WLS feed water

Synthesis of ITO NPs

The ITO NPs were prepared following the procedure outlined in our previous study [30]. In summary, $InCl_3$ and $SnCl_4$, with a molar ratio of ten to one for indium and tin, were first reacted in an aqueous solution containing NH_4OH to produce a mixture of SnO_2-In $(OH)_3$ and NH_4Cl. After several centrifuging/washing cycles (for eliminating the NH_4Cl), the resulting white SnO_2-In $(OH)_3$ compound (Figure 1a) was treated at 700°C for crystallization and removal of excess water, where yellow ITO powder was generated (Figure 1b). Finally, the yellow crystals were hydrogenated in a tube furnace at 350 °C to yield blue conductive ITO NPs (Figure 1c). Figure 1d shows the X-ray powder diffraction (XRD) profile and high resolution scanning electron microscopy (SEM) image of the synthesized ITO NPs. The size of the NPs was obtained to be 15±0.3 nm using the Debye Scherer equation [29].

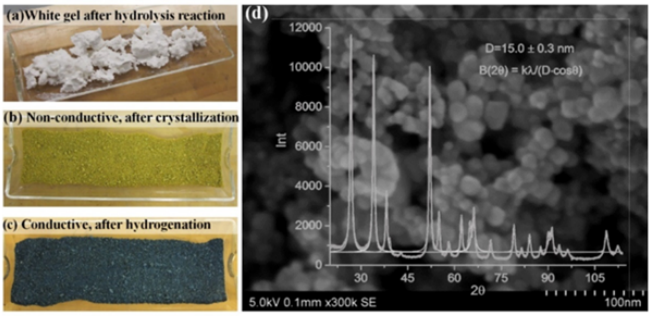

Figure 1. (a) White SnO_2-$In(OH)_3$ compound synthesized with the reaction of $InCl_3$ and $SnCl_4$ in the presence of NH_4OH, followed by centrifuging and washing of reaction product; (b) Synthesized yellow ITO crystals after crystallization of SnO_2-$In(OH)_3$ compound at 700 °C; (c) Conductive blue ITO crystals after hydrogenation with gas streams of 10%/90% H_2/Ar; (d) XRD and FESEM of the ITO NPs.

Fabrication of TFC and TFN membrane

The composite membranes were fabricated by interfacial polymerization (IP) reaction using an aqueous MPD solution and an organic-TMC solution, as shown schematically in Figure 2. First, the PES support was mounted onto a plexiglass frame, and then an aqueous solution containing MPD (2 wt.%), TEA (1 wt.%), CSA (2 wt.%), and SDS (0.2 wt%) was poured on the surface of PES support. After a soaking time of 8 minutes, the excess aqueous solution was removed. Then, 0.2 wt.% TMC solution was poured over the MPD-impregnated PES support to allow the polymerization reaction to proceed for 30 seconds. Finally, to remove the residual organic solvent, the membrane was dried for 4 minutes in an air circulated oven at 60 ºC. The fabrication procedure of the TFN membranes is shown in Figure 3. First, a mother NP suspension was prepared by dispersing 0.6 g ITO, and 150 µl BYK106 in 30 ml heptane solution based on an optimal synthesis step, reported in our previous work [30]. Then, two different volumes of 1 ml and 2 ml from the mother suspension were added to the TMC-heptane solution and agitated for 4 minutes in a bath sonicator. The prepared ITO-TMC solution was employed in IP reaction to prepare ITO-modified TFN membranes. The TFN membranes were labeled as TFN1 and TFN2, which were synthesized using the dose of 1 ml and 2 ml of the ITO NP suspension in the TMC solution, respectively.

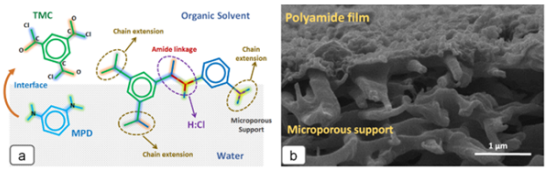

Figure 2. (a) illustration of interfacial polymerization reaction between MPD and TMC monomers, (b) cross-sectional images of the TFC membrane having a thin polyamide layer over a porous support membrane.

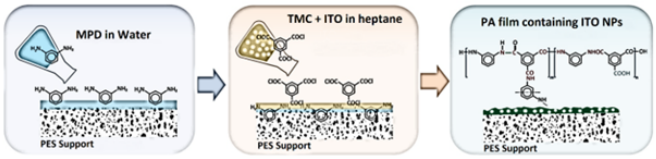

Figure 3. The fabrication of TFN membranes via adding ITO NPs during IP reaction

Characterization of membranes physicochemical properties

The surface morphology of the membranes was analyzed using field

emission scanning electron microscopy (FESEM, Zeiss Sigma, Germany). The cross section of the membranes was observed using transmission electron microscopy (TEM, Philips/FEI Morgagni, The Netherlands). The chemical composition of the membranes was analyzed using energy dispersive X-ray (EDX) spectroscopy (Bruker, Billerica, Massachusetts, USA). The surface wettability of the membranes was characterized using a drop shape analyzer (Krüss, Hamburg, Germany). A stripe of membrane sample was placed on a microscope slide, and a drop of DI water was placed on the active (polyamide) side of the membrane. The drop was allowed to rest for 30 seconds to ensure the equilibrium contact angle was reached. The test was repeated four times at different locations of the sample, and the average data was reported. The zeta potential of the membranes was measured by an electrokinetic analyzer (SurpassTM 3, Anton Parr, Graz, Austria). Thermal gravimetric analysis (TGA) was conducted on the fabricated membranes to measure their thermal stability. TGA measures the change in weight of the sample in relation to a changing temperature. 10 mg of the membrane sample was placed in the sample holder of the TGA Q50 (TA Instrument, Newcastle, Delaware, USA). The temperature was then increased to 700°C with a rate of 10°C/min, and the change in weight of the samples was recorded. Based on the literature, the decomposition temperature of the TFN membrane was defined as the temperature after a 3% weight loss [35].

Characterization of permeation performance of the membranes

The synthesized membranes were tested in RO crossflow filtration setup (Sterlitech Co, WA, USA). The performance of membranes was evaluated at steady state with a transmembrane pressure of 220 psi, and a feed flow rate of 1 $Lmin^{-1}$ at 25 °C. Equation 1 was used to calculate the water flux (J_w).

$$J_w = \left(\frac{\Delta m}{\rho A_m \Delta t}\right)$$

where Δm is the mass of the permeate water over the measurement time (Δt), divided by the effective surface area of the membrane (A_m). The salt rejection percentage (R) was obtained using Equation 2.

$$R = \left(1 - \frac{C_p}{C_f}\right) \times 100$$

The salt concentrations of permeate water (C_p) and the feed solution (C_f) were measured using a conductometer (Accumet AR50, Fisher Scientific).

Characterization of the antifouling properties of the membranes

Fouling tests were conducted using the RO filtration setup. WLS feed water was filtered for 360 min at different transmembrane pressures to obtain a similar initial flux (25 LMH) for all membranes. The total organic carbon (TOC) and the total dissolved solids (TDS) of the permeate (Cp) were measured at the end of filtration. The rejection percentage of TOC and TDS was measured using Equation 2, and the TOC and TDS of feed solution (C_f) were presented in Table 1. Also, three commercial membranes, namely Hydranautics NF ESNA, RO ESPA, and FilmTec NF270, were used for benchmarking our synthesized membranes. The properties of these membranes are provided in detail elsewhere [36].

Results and Discussion

Comparison of the morphologies of the membranes

Figure 4 illustrates the backscattered electron image and the EDX elemental composition of the surfaces of the membrane. The tables in the insets d-f show that the addition of ITO NPs increased the weight percentage of indium and tin elements from 0% for the unmodified TFC membrane to 26% and 0.5% for TFN1, and 43% and 5.6% for TFN2 membrane. This observation confirms the successful incorporation of the ITO NPs into the polyamide layer of the composite membranes. Higher magnification SEM images of the top surface are presented in Figure 5. As shown, the ITO NPs cover the typical ridge and valley structure of TFC membranes in Figure 5a.

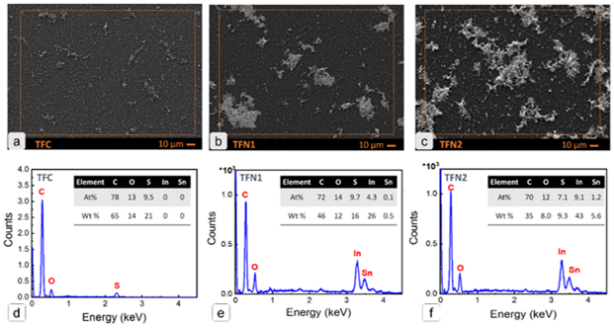

Figure 4. (a-c) Surface backscattered electron image, and (d-f) EDX elemental composition of the control TFC, TFN1, and TFN2 membranes. The higher weight percentages of the indium and tin elements in TFN1 and TFN2 membranes showed the successful incorporation of the ITO NPs in the membranes' active layer.

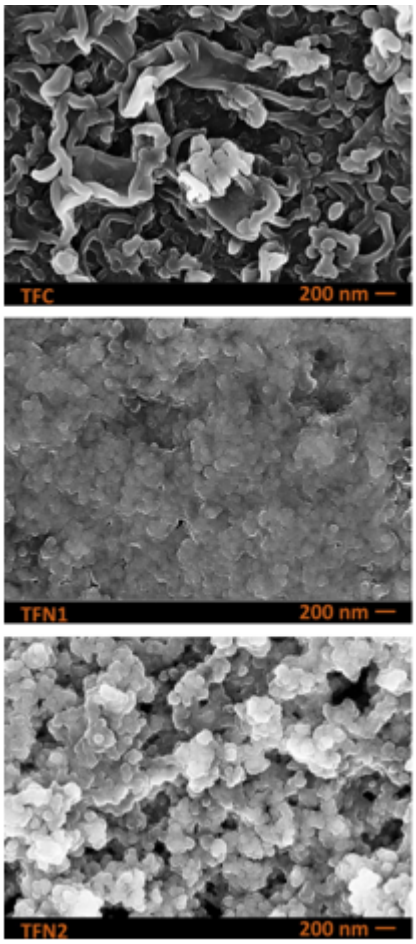

Figure 5. FESEM images of the pristine TFC, TFN1, TFN2 membranes at a magnification of 20,000X

The cross sectional TEM images of the membranes (Figure 6) also confirm the presence of the ITO NPs in the top PA layer. The TEM images illustrate that the ITO NPs were incorporated to the topmost part of the polyamide, where the membrane is in contact with the feed solution. Furthermore, the overall thickness of the polyamide layer was increased by the addition of ITO NPs from the base TFC membrane to TFN2. This observation can be connected to (i) the reduction in the concentration of TMC monomers

by adding ITO NPs suspension and (ii) an increase in the BYK106 concentration with the addition of the ITO-heptane suspension. A decrease in the TMC concentration might have led to the formation of a looser incipient polyamide layer at the early stage of the interfacial polymerization reaction. This would have resulted in less resistance toward diffusion of the MPD molecules towards the organic solvent and thus increased the polyamide layer's overall thickness [37]. Also, the BYK106 molecules could have decreased the interfacial tension between the aqueous and organic monomer solutions, allowing for faster transport of MPD molecules to the reaction zone at the interface [38]. Higher magnification TEM images in Figure 7 show that ITO NPs were entrapped in the polyamide matrix to a certain depth, implying their firm attachment to the surface and robustness of fabricated TFN membranes.

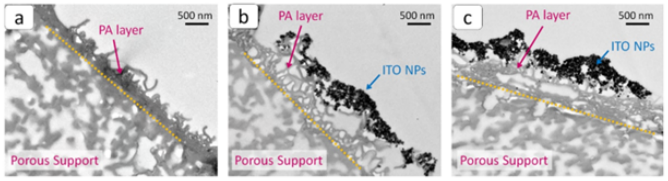

Figure 6. TEM images of (a) base TFC, (b) TFN1, and (c) TFN2 membranes (22,000X magnification). The dashed line distinguishes the active polyamide layer from the PES sublayer. The black spots in the polyamide layer are ITO NPs.

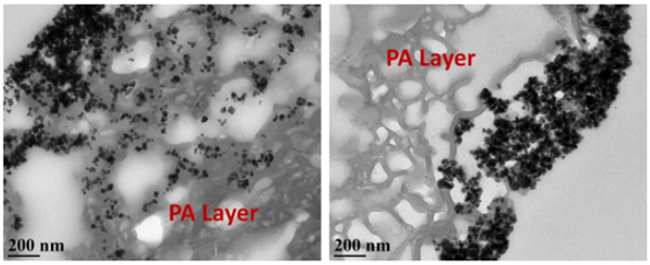

Figure 7. Higher magnification TEM cross-sectional images (56,000X magnification) of TFN2.

Surface wettability and the electrical potential of the membranes

The water contact angles of the ITO TFN membranes and the base polyamide TFC membrane are shown in Figure 8a. The addition of ITO NPs increased the surface wettability of the membrane, as shown by a significant decrease in contact angle from ~82^{O}C for the TFC membrane to ~65^{O}C for TFN2. The higher surface wettability of the ITO nanocomposite membranes can be ascribed to the greater affinity of water molecules to the ITO NPs. The addition of these metal oxides provided favorable spots for hydrogen bonding and thus diffusion of water molecules through the polyamide layer [39]. The contact angle results suggest that the ITO-modified membranes can potentially provide better antifouling properties, as the enhanced wettability of the membrane toward water decreases the attachment of foulants, especially organic matter, to the surface of the membranes [40].

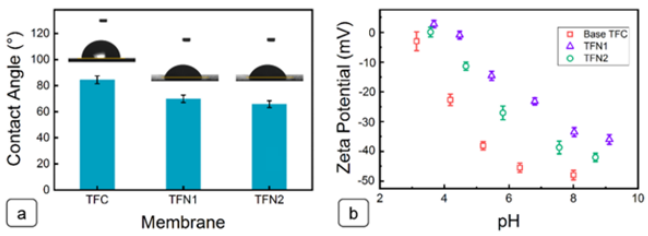

Figure 8. (a) Surface wettability and (b) surface potential of the synthesized membranes. The incorporation of ITO NPs into the polyamide layer increased the surface wettability and made the resulting membrane less negatively charged.

The addition of ITO NPs was observed to decrease the value of the surface potential and made the modified membranes less negative for all pH values (Figure 8b). The decreasing trend of the zeta potential of the synthesized membranes with pH is likely due to the protonation/deprotonation of carboxylic acids and amine groups present on the surface [36,41,42]. At low pH values, the protonation of amine groups results in a more positively charged surface. Conversely, the more negative charge at higher pH originates from the deprotonation of the amine groups as well as the dissociation of the carboxylic acid groups. The lower surface potential of the TFN membranes than the base TFC membrane can be attributed to the positive charge of ITO NPs [30]. A less negatively charged membrane may be beneficial for the retention of positive divalent ions such as magnesium and calcium. When attached to the surface, these divalent ions can act as a bridge between the organic matter such as humic acids and alginate molecules and facilitate their deposition onto the membrane surface [43]. Therefore, the less attachment of these divalent ions, due to the increased electrostatic repulsion, can play a crucial role in reducing scaling and organic fouling during seawater desalination and industrial wastewater treatment [43].

Thermal stability of membranes

Figure 9 shows the result of the TGA analysis of the pristine TFC and TFN2 membranes. The results show that loading 0.02% ITO NPs was enough to increase the degradation temperature of the TFC membrane from 455°C to 472°C. The largest weight loss difference occurred at 590°, where the ITO TFN membrane was able to retain 12% more of its original weight than the TFC membrane. Based on the literature, the addition of NPs to polymeric membranes reduces the polymer chain mobility and thus increases the thermal stability of membranes [35].

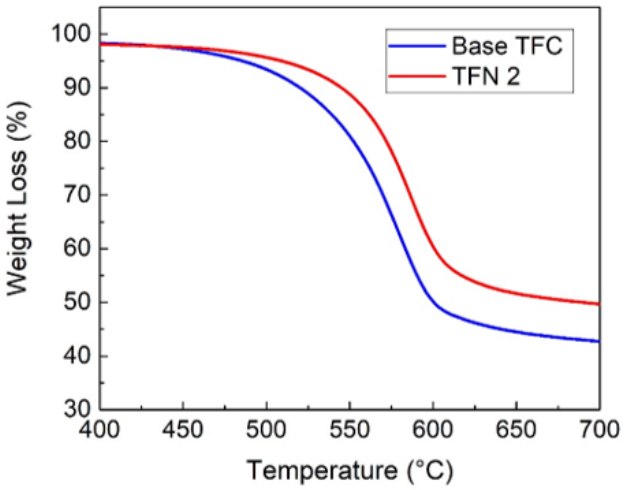

Figure 9. Weight loss of TFC and TFN2 membranes as a function of temperature

Permeation performance of the membranes in RO process

Table 2 presents the pure and saline water permeation and salt removal performance of the membranes in the RO process. By loading the ITO NPs, the water flux increased significantly from ~27.7 LMH for the base TFC membrane to ~48.0 LMH for the TFN3 membrane. The addition of salt to the feed solution was shown to drop the flux of the membranes due

to the concentration polarization effect. Furthermore, the enhancement of the water flux resulted in negligible reduction (~1%) in salt rejection of the membranes from ~98.0% to ~97.0% revealing that the addition of the ITO NPs did not cause any defects in the polyamide layer.

Membrane	Pure Water Flux (LMH)	Saline Water Flux (LMH)	Salt Rejection (%)
TFC	27.7 ± 0.7	25.3 ± 0.7	98.0 ± 0.2
TFN1	36.0 ± 1.0	34.5 ± 1.0	97.7 ± 0.2
TFN2	48.0 ± 1.2	43.5 ± 1.1	97.0 ± 0.2

Table 2. Permeation performance of the prepared membranes in the RO process

Fouling characteristic of the membranes

Figure 10 presents the fouling characteristics of the lab synthesized TFC and TFN membranes as well as three commercial membranes by WLS feed water. The transmembrane pressure for each test was adjusted to conduct all experiments at the same initial flux. This allows attributing the changes in permeation properties to the membrane material, not the hydrodynamic condition [29]. As can be seen in Figure 10, the integration of ITO NPs into the polyamide layer effectively decreased the required transmembrane pressure from 300 psi for the base TFC to 150 psi, and 120 psi for the TFN1 and TFN2 membranes, respectively, to achieve 25 LMH flux. The significant reduction in the transmembrane pressure was achieved by a slight sacrifice in the TOC and TDS rejection. The removal of TDS and TOC from WLS feed water decreased from 97% in base TFC membrane to 95% and 93% for TFN2, respectively.

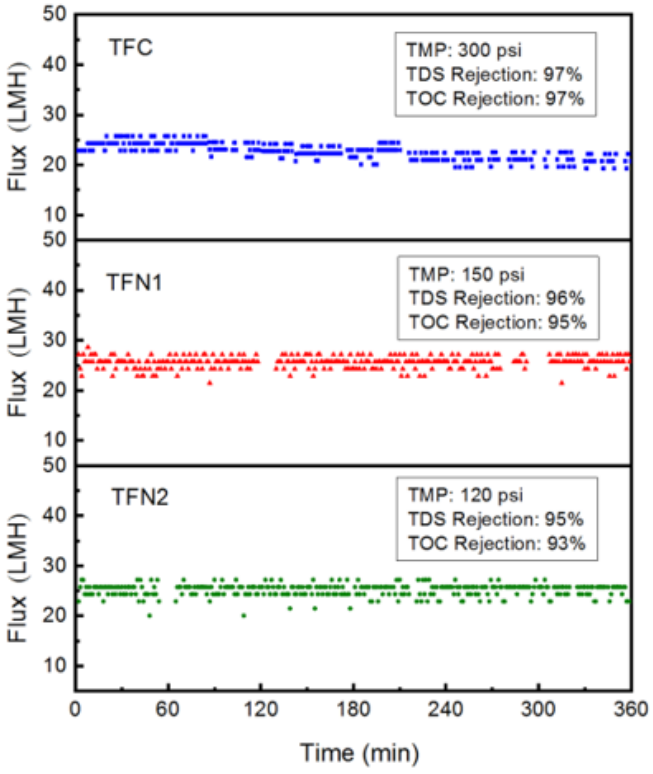

Figure 10. Fouling characteristics and TOC and TDS removal percentage of lab-synthesized TFC and TFN membranes. The transmembrane pressure was adjusted to conduct all the experiments at the same initial flux of 25 LMH.

At the same pressure, the Hydranautics ESPA membrane provided 91% and 92% rejection for TDS and TOC, respectively (Figure 11). Although the NF270 and ESNA membranes required lower transmembrane pressure (60 psi and 100 psi, respectively), their TDS and TOC removal performance decreased significantly, especially for NF270. Moreover, the water flux remained constant for the lab synthesized TFN membranes, while a gradual decrease in the permeation flux of the pristine TFC and commercial membranes was observed over time. The flux decline was more severe for ESNA and ESPA membranes that showed almost 20% and 24% flux decline, respectively, over the filtration time.

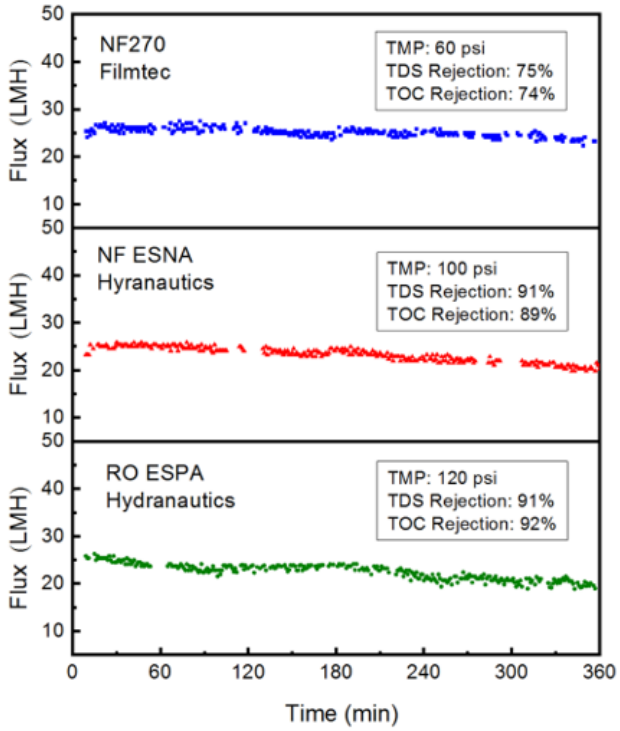

Figure 11. Fouling characteristics and TOC, and TDS removal percentage of commercial NF270, ESNA, and ESPA membranes. The transmembrane pressure was adjusted to conduct all the experiments at the same initial flux of 25 LMH.

Conclusion

In the present study, we integrated ITO NPs into the polyamide layer of a TFC membrane to enhance its permeation and antifouling properties. The synthesized ITO-TFN membranes demonstrated superior water flux compared to the pristine TFC membrane without a significant reduction in salt removal. Furthermore, the ITO-modified TFN membranes demonstrated enhanced fouling resistance owing primarily to their improved surface wettability toward water compared to base TFC membrane when tested with WLS feed water of the SAGD process. The present study presents the promising application of ITO NPs to develop novel energy efficient nanocomposite membranes with enhanced permeation and antifouling performance. It is suggested as a continuation of this study to evaluate the impact of higher concentrations of ITO NPs on the permselectivity, high temperature resistance, and electrical conductivity of the ITO-TFN membranes. This objective needs appropriate tuning of the interfacial polymerization reaction in terms of the concentrations of ITO NPs, the

reacting monomers, and the chemical additives to fabricate robust and defect free TFN membranes.

Acknowledgment

The authors gratefully appreciate the financial support from the Natural Sciences and Engineering Research Council of Canada (NSERC), Suncor Energy, Devon Energy, and ConocoPhillips.

Author contributions

B.K. and Z.A conducted the experiments, analyzed and validated the data, and wrote the original draft. G.M. synthesized and characterized the ITO nanoparticles. M.S. reviewed and edited the manuscript and played an advisory role. All authors contributed to the writing of the manuscript.

Competing Interests

The authors declare no competing interests.

Data accessibility statement

All data generated or analyzed during this study are included in this published article.

References

1. "Global Risks Report." World Economic Forum (2019).
2. Elimelech, M. "The global challenge for adequate and safe water." J. Water Supply Res. Technol - AQUA (2006) 55: 3–10.
3. "Factsheet on drinking water." World Health Organization (2019).
4. Shannon, MA. "Science and technology for water purification in the coming decades". Nature (2008) 452: 301–10.
5. Motsa, MM, Mamba BB, D'Haese A and Hoek EMV, et al. "Organic fouling in forward osmosis membranes: The role of feed solution chemistry and membrane structural properties." J. Memb. Sci (2014) 460: 99–109.
6. Li, D and Wang H. "Recent developments in reverse osmosis desalination membranes." J. Mater. Chem (2010) 20: 4551.
7. Wang, Z, Jiang X, Cheng X and Lau CH, et al. "Mussel-inspired hybrid coatings that transform membrane hydrophobicity into high hydrophilicity and underwater superoleophobicity for oil-in-water emulsion separation." ACS Appl. Mater. Interfaces (2015) 7: 9534–9545.
8. Khorshidi, B, Bhinder A, Thundat T and Pernitsky DJ, et al. "Developing high throughput thin film composite polyamide membranes for forward osmosis treatment of SAGD produced water." J. Memb. Sci (2016) 511: 29–39.
9. Khorshidi, B, Soltannia B, Thundat T and Sadrzadeh M. "Synthesis of thin film composite polyamide membranes: Effect of monohydric and polyhydric alcohol additives in aqueous solution." J. Memb. Sci (2017) 523: 336–345.
10. Karami, P, Khorshidi B, Soares JBP and Sadrzadeh M. "Fabrication of highly permeable and thermally-stable reverse osmosis thin film composite polyamide membranes." ACS Appl. Mater. Interfaces (2020) 12: 2916–2925.
11. Karami, P. "Thermally stable thin film composite polymeric membranes for water treatment: A review." J. Clean. Prod (2019): 119447.
12. Rastgar, M. "Removal of trace organic contaminants by melamine-tuned highly cross-linked polyamide TFC membranes." Chemosphere (2020) 238: 124691.
13. Caseri, WR. "Nanocomposites of polymers and inorganic particles: Preparation, structure and properties." Mater. Sci. Technol (2006) 22: 807–817.
14. Ng, LY, Mohammad AW, Leo CP and Hilal N. "Polymeric membranes incorporated with metal/metal oxide nanoparticles: A comprehensive review." Desalination (2013) 308: 15–33.
15. Paul, DR and Kemp DR. "The diffusion time lag in polymer membranes containing adsorptive fillers." J. Polym. Sci. Polym. Symp (1973) 41: 79–93.
16. Jeong BH. "Interfacial polymerization of thin film nanocomposites: A new concept for reverse osmosis membranes." J. Memb. Sci (2007) 294: 1–7.
17. Nguyen, A, Zou L and Priest C. "Evaluating the antifouling effects of silver nanoparticles regenerated by TiO_2 on forward osmosis membrane." J. Memb. Sci (2014) 454: 264–271.
18. Yu, B, Leung KM, Guo Q and Lau WM, et al. "Synthesis of Ag–TiO 2 composite nano thin film for antimicrobial application." Nanotechnology (2011) 22: 115603.
19. Khorshidi, B, Biswas I, Ghosh T and Thundat T, et al. "Robust fabrication of thin film polyamide-TiO_2 nanocomposite membranes with enhanced thermal stability and anti-biofouling propensity." Sci. Rep (2018) 8: 784.
20. Pendergast, MM and Hoek EMV. "A review of water treatment membrane nanotechnologies." Energy Environ. Sci (2011) 4: 1946.
21. Das, R. "Multifunctional carbon nanotubes in water treatment: The present, past and future." Desalination (2014) 354: 160–179.
22. Hegab, HM and Zou L. "Graphene oxide-assisted membranes: Fabrication and potential applications in desalination and water purification." J. Memb. Sci (2015) 484: 95–106.
23. Qu, X, Alvarez PJJ and Li Q. "Applications of nanotechnology in water and wastewater treatment." Water Res (2013) 47: 3931–46.
24. Hernandez, S, Saad A, Ormsbee L and Bhattacharyya D. "Nanocomposite and Responsive Membranes for Water Treatment in Emerging Membrane Technology for Sustainable Water Treatment." Elsevier Science (2016): 389–431.
25. Al Aani, S, Wright CJ, Atieh MA and Hilal N. "Engineering nanocomposite membranes: Addressing current challenges and future opportunities." Desalination (2017) 401: 1–15.
26. Bassyouni, M, Abdel-Aziz MH, Zoromba MS and Abdel-Hamid, et al. "E. A review of polymeric nanocomposite membranes for water purification." J. Ind. Eng. Chem (2019) 73: 19–46.
27. Khorshidi, B, Shabani S and Sadrzadeh M. "Prospects of nanocomposite membranes for water treatment by osmotic-driven membrane processes in Nanocomposite Membranes for Water and Gas Separation." Elsevier Inc (2020): 257–297.
28. Shabani, S, Khorshidi B and Sadrzadeh M. "Development of nanocomposite membranes by biomimicking nanomaterials." Nanocomposite Membr. Water Gas Sep (2020): 219–236.
29. Khorshidi, B, Hajinasiri J, Ma G and Bhattacharjee S, et al. "Thermally resistant and electrically conductive PES/ITO nanocomposite membrane." J. Memb. Sci (2016) 500: 151–160.
30. Almansoori, Z, Khorshidi B, Sadri B and Sadrzadeh M. "Parametric study on the stabilization of metal oxide nanoparticles in organic solvents: A case study with indium tin oxide (ITO) and heptane." Ultrason. Sonochem (2018) 40: 1003–1013.
31. Sadrzadeh, M, Pernitsky DJ and Mcgregor M. "Nanofiltration for the Treatment of Oil Sands-Produced Water in Nanofiltration." InTech (2018): 25–45.
32. Mohammadtabar, F, Pillai RG, Khorshidi B and Hayatbakhsh A, et al. "Efficient treatment of oil sands produced water: Process integration using ion exchange regeneration wastewater as a chemical coagulant." Sep. Purif. Technol (2019) 221: 166–174.
33. Shamaei, L, Khorshidi B, Perdicakis B and Sadrzadeh M. "Treatment of oil sands produced water using combined electrocoagulation and chemical coagulation techniques." Sci. Total Environ (2018) 645: 560–572.
34. Pillai, RG. "Characterization and comparison of dissolved organic matter signatures in steam-assisted gravity drainage process water samples from Athabasca oil sands." Energy and Fuels (2017) 31: 8363–8373.
35. Li, JF, Xu ZL, Yang H and Yu LY, et al. "Effect of TiO_2 nanoparticles on the surface morphology and performance of microporous PES membrane." Appl. Surf. Sci (2009) 255: 4725–4732.
36. Hayatbakhsh, M, Sadrzadeh M, Pernitsky D and Bhattacharjee S, et al. "Treatment of an in situ oil sands produced water by polymeric membranes." Desalin. Water Treat (2016) 57: 14869–14887.
37. Khorshidi, B, Thundat T, Fleck B and Sadrzadeh M. "Thin film composite polyamide membranes: Parametric study on the influence of synthesis conditions." RSC Adv (2015) 5: 54985–54997.
38. Khorshidi, B, Thundat T, Pernitsky D and Sadrzadeh M. "A parametric study

on the synergistic impacts of chemical additives on permeation properties of thin film composite polyamide membrane." J. Memb. Sci (2017) 535: 248–257.

39. María Arsuaga, J. "Influence of the type, size and distribution of metal oxide particles on the properties of nanocomposite ultrafiltration membranes." J. Memb. Sci (2013) 428: 131–141.

40. Ismail, MF, Khorshidi B and Sadrzadeh M. "New insights into the impact of nanoscale surface heterogeneity on the wettability of polymeric membranes." J. Memb. Sci (2019) 590: 117270.

41. Sadrzadeh, M, Hajinasiri J, Bhattacharjee S and Pernitsky D. "Nanofiltration of oil sands boiler feed water: Effect of pH on water flux and organic and dissolved solid rejection." Sep. Purif. Technol (2015) 141: 339–353.

42. Lau, WJ, Ismail AF, Goh PS and Hilal N, et al. "S. Characterization methods of thin film composite nanofiltration membranes." Sep. Purif. Rev (2015) 44: 135–156.

43. Resosudarmo, A, Ye Y, Le-Clech P and Chen V. "Analysis of UF membrane fouling mechanisms caused by organic interactions in seawater." Water Res (2013) 47: 911–921.

How to cite this article: Guibin Ma, Zayed Almansoori, Behnam Khorshidi and Mohtada Sadrzadeh. "Development of antifouling thin-film nanocomposite polyamide membrane using ITO nanoparticles." J Material Sci Eng 10 (2021): 01-07